

**Daria Gushchina<sup>1</sup>, Florian Heimsch<sup>2</sup>, Alexander Osipov<sup>1</sup>, Tania June<sup>3</sup>, Abdul Rauf<sup>4</sup>, Heiner Kreilein<sup>2</sup>, Oleg Panferov<sup>5</sup>, Alexander Olchev<sup>1\*</sup>, Alexander Knohl<sup>2</sup>**

<sup>1</sup> Faculty of Geography, Moscow State University, Moscow, Russia

<sup>2</sup> Bioclimatology, University of Goettingen, Goettingen, Germany

<sup>3</sup> Bogor Agricultural University, Department of Geophysics and Meteorology, Bogor, Indonesia

<sup>4</sup> Universitas Tadulako, Palu, Indonesia

<sup>5</sup> Department of Climatology and Climate Protection, Faculty of Life Sciences and Engineering, University of Applied Sciences, Bingen am Rhein, Germany

\* **Corresponding author:** aoltche@gmail.com

# EFFECTS OF THE 2015–2016 EL NIÑO EVENT ON ENERGY AND CO<sub>2</sub> FLUXES OF A TROPICAL RAINFOREST IN CENTRAL SULAWESI, INDONESIA

**ABSTRACT.** The influence of the very strong 2015–16 El Niño event on local and regional meteorological conditions, as well as on energy and CO<sub>2</sub> fluxes in a mountainous primary tropical rainforest was investigated using ERA-Interim reanalysis data as well as meteorological and eddy covariance flux measurements from Central Sulawesi in Indonesia. The El Niño event led to a strong increase of incoming monthly solar radiation and air temperature, simultaneously with the increasing Niño4 index. Monthly precipitation first strongly decreased and then increased reaching a maximum in 3–4 months after El Niño culmination. Ecosystem respiration increased while gross primary production showed only a weak response to the El Niño event resulting in a positive anomaly of net ecosystem CO<sub>2</sub> exchange (reduced CO<sub>2</sub> uptake). The changes of key meteorological parameters and fluxes caused by the strong El Niño event of 2015–16 differed from the effects of moderate El Niño events observed during the period 2003–2008, where net ecosystem CO<sub>2</sub> exchange remained largely unaffected. In contrast to earlier moderate El Niño events, the strong El Niño 2015–16 affected mostly the air temperature resulting in a weakening of the net carbon sink at the rainforest site in Central Sulawesi, Indonesia.

**KEY WORDS:** El Niño Southern Oscillation, Niño4, tropical rainforest, eddy covariance flux measurements, energy and CO<sub>2</sub> fluxes

**CITATION:** Daria Gushchina, Florian Heimsch, Alexander Osipov, Tania June, Abdul Rauf, Heiner Kreilein, Oleg Panferov, Alexander Olchev, Alexander Knohl (2019) Effects Of The 2015–2016 El Niño Event On Energy And CO<sub>2</sub> Fluxes Of A Tropical Rainforest In Central Sulawesi, Indonesia. *Geography, Environment, Sustainability*, Vol.12, No 2, p. 183–196  
DOI-10.24057/2071-9388-2018-88

## INTRODUCTION

The contribution of tropical rainforests to the global budget of atmospheric greenhouse gases (GHG), their possible influence on the climate system and their sensitivity to environmental changes are key topics of numerous modeling and experimental studies (Grace et al. 1995; Malhi et al. 2007, 2010; Le Quére et al. 2015). Tropical forests cover large areas of the Earth's surface and they are characterized by a large diversity. Their growth and development are governed by various factors including the regional climatic conditions, landscape properties and soil characteristics (FAO 2016). Representative information about possible responses of tropical forest ecosystems to changing environmental conditions can help to obtain new knowledge about possible future dynamics of tropical forest ecosystems in different geographical regions as well as to describe the possible effects of vegetation and land-use changes in tropical regions on local and regional climate conditions.

South-East (SE) Asia hosts some of the oldest, intact rainforests on Earth (Corlett and Primack 2006). They still cover vast areas in the region and are characterized by a large biological diversity and high species richness (Myers et al. 2000). A high deforestation rate due to widespread logging over the last decades in the region leads, however, to degradation of the primary rainforests and to reduction of their extension (FAO 2016; Hansen et al. 2013). During the last decades, rainforest in SE Asia were the objects of intensive aggregated studies of ecosystem - atmosphere interactions (Ibrom et al. 2007; Ichii et al. 2017). Nevertheless, considerable parts of primary tropical rainforests in remote areas, far away from administrative centers and human settlements, are still very poorly investigated in respect to their sensitivity to changes of environmental conditions and their contributions to the global and regional budgets of GHG in the atmosphere.

Recent scientific assessments indicated that the tropical rainforests of SE Asia are highly sensitive to the effects of large-scale

atmospheric and oceanic modes such as El Niño-Southern Oscillation, Indian Ocean Dipole, Madden-Julian Oscillation (Hirano et al. 2007; Olchev et al. 2015). El Niño-Southern Oscillation (ENSO) is associated with quasi-periodic fluctuations in sea surface temperature (SST) in the central and eastern parts of the Equatorial Pacific and atmospheric pressure fluctuations between the eastern and western tropical Pacific. It has significant influence on the weather and climatic conditions both in the tropical Pacific region and through teleconnections at mid and high latitudes (Trenberth et al. 1998; Diaz et al. 2001; Zheleznova and Gushchina 2015, 2016). The warm phase (or event) of ENSO, termed El Niño, is characterized by positive SST anomalies located either in the Eastern (conventional event) or Central (Modoki event) Pacific (Ashok et al. 2007). The ocean warming is associated with a well pronounced shift of the Walker circulation to the east, resulting in strong convection and abundant precipitation over the Central and Eastern Pacific as well as in decreasing cloudiness and precipitation in Western Pacific areas, including the islands of the Indonesian archipelago and Northern and Eastern Australia (Gushchina et al. 1997; Dewitte et al. 2002). The decreasing cloudiness in the Western Pacific leads to increased solar radiation and air temperature.

To describe possible effects of ENSO events on  $\text{CO}_2$ - and  $\text{H}_2\text{O}$ -exchange between the land surface and the atmosphere, studies for various Western Pacific regions were carried out during the last decades (Feely et al. 1999; Olchev et al. 2015). Most of them, however, analyzed relatively weak El Niño events due to the absence of strong El Niño events between 1998 and 2015.

The main goal of this study is therefore to describe possible effects of the very strong 2015–2016 El Niño event (warm phase of ENSO) on energy, water, and  $\text{CO}_2$  fluxes in the Western Pacific at the example of mountainous old-growth tropical rainforest growing in Central Sulawesi, Indonesia.

## MATERIAL AND METHODS

### Study area

The tropical rainforest selected for the study is situated near the village Bariri in the southern part of the Lore Lindu National Park in Central Sulawesi in Indonesia (1°39.47'S and 120°10.41'E or UTM 51S 185482.0 m East and 9816523.0 m North) (Fig. 1). The site is located on a large plateau with a size of several kilometers, about 1440 m above sea level. The area is surrounded by mountain chains surmounting the plane by another 300 m to 400 m. A 70 m high micrometeorological tower is installed on the site and equipped with meteorological and gas-exchange measuring sensors. Within 500 m around the tower the elevation varies between 1390 and 1430 meters (Ibrom et al. 2007; Olchev et al. 2015).

The area is influenced by the intertropical convergence zone (ITCZ) and it is characterized by a humid climate with low temperature range throughout the year (the mean monthly air temperature varies between 19.4°C and 19.7°C). It belongs to

the tropical wet (or rainforest) climate (Af) according to the Köppen-Geiger climate classification (Chen and Chen 2013; Olchev et al. 2015) and to the equatorial type of climate - according to the climate classification suggested by Alisov (Alisov 1954). The mean annual precipitation rate exceeds 2000 mm with May to October exhibiting drier conditions than the rest of the year (Ibrom et al. 2007; Olchev et al. 2015).

The vegetation cover at the site is characterized by a large diversity. There are more than 90 different tree species per hectare (Ibrom et al. 2007). Among the dominant species are *Castanopsis accuminatissima* BL. (29%), *Canarium vulgare* Leenh. (18%) and *Ficus* spec. (9.5%). The density of trees, with diameter at breast height (DBH) larger than 0.1 m, is about 550 trees ha<sup>-1</sup>. Additionally there is more than a 10-fold larger number of smaller trees with a stem diameter lower than 0.1 m. Leaf area index (LAI) is about 7.2 m<sup>2</sup> m<sup>-2</sup>. LAI was estimated using an indirect hemispherical photography method. The height of the trees, with DBH >0.1 m, varies between 12 m and 36 m with the mean of 21 m (Ibrom et al. 2007).

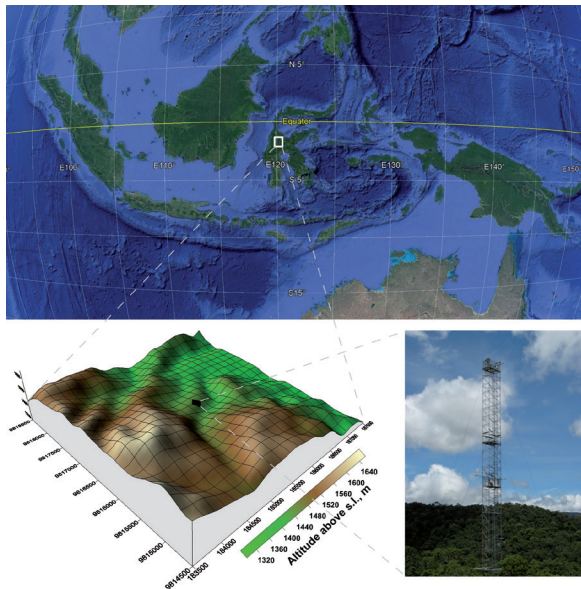


**Fig. 1. Geographical location (source: Google maps), surface topography of the Bariri site and a photo of the meteorological tower for long-term observations of the energy, water, and CO<sub>2</sub> fluxes between land surface and the atmosphere. The surface topography map was created using ASTER GDEM version 2 data set (<https://asterweb.jpl.nasa.gov/gdem.asp>)**

## Reanalysis data

Various reanalysis products are used to document the anomalies of meteorological and oceanic parameters observed in the study area during the 2015–16 El Niño. Monthly net solar radiation, air temperature and wind at the 850 hPa level are obtained from the ERA-Interim reanalysis (Dee et al. 2011) with the grid spacing of  $2.5^\circ \times 2.5^\circ$ . To derive monthly SST the Extended Reconstructed Sea Surface Temperature version 4 (ERSST.v4) archive is used (grid spacing of  $2^\circ \times 2^\circ$ ). Precipitation anomalies are calculated from the GPCP archive (Huffman et al. 2009), with the grid spacing of  $2.5^\circ \times 2.5^\circ$ . Anomalies are calculated respectively to the mean seasonal cycle averaged over 1979–2014 period. Niño3 (SST anomalies averaged over  $150^\circ\text{W}$ – $90^\circ\text{W}$  and  $5^\circ\text{S}$ – $5^\circ\text{N}$ ) and Niño4 (SST anomalies averaged over  $160^\circ\text{E}$ – $150^\circ\text{W}$  and  $5^\circ\text{S}$ – $5^\circ\text{N}$ ) indices are obtained from [https://www.esrl.noaa.gov/psd/gcos\\_wgsp/Timeseries/](https://www.esrl.noaa.gov/psd/gcos_wgsp/Timeseries/).

## Flux measurements in the tropical rainforest

Measurements of  $\text{CO}_2$  and  $\text{H}_2\text{O}$  fluxes are carried out at the Bariri site since 2003 (Falk et al. 2005; Ibrom et al. 2007, 2008; Panferov et al. 2009). Eddy covariance equipment for flux measurements is installed on a meteorological tower of 70 m height at the 48 m level, i.e. ca. 12 m above the maximum tree height. The measuring system consists of a three-dimensional sonic anemometer (USA-1, Metek, Germany) and an open-path  $\text{CO}_2$  and  $\text{H}_2\text{O}$  infrared gas analyzer (IRGA, LI-7500A, Li-Cor, USA). The system is solar powered and entirely self-sustaining. It has been proven to run unattended over a period of several months. Post-field data processing of eddy covariance flux estimates was carried out strictly according to established recommendations for raw data analysis including despiking, block averaging, and 2D coordinate rotation (Aubinet et al. 2012). Negative fluxes indicate a flux towards the land surface (uptake), positive fluxes a flux towards the atmosphere (release). For filling the gaps in the measured Net Ecosystem Exchange (*NEE*), sensible and latent heat flux records as well as to

quantify Gross Primary Production (*GPP*), Net Primary Production (*NPP*) and Ecosystem respiration (*RE*) the process-based Mixfor-SVAT model (Olchev et al. 2002; 2008, 2015) was used.

Mixfor-SVAT is a one-dimensional model of the energy,  $\text{H}_2\text{O}$  and  $\text{CO}_2$  exchange between vertically structured mono- or multi-specific forest stands and the atmosphere. The key advantage of the model is its ability to describe seasonal and daily patterns of  $\text{CO}_2$  and  $\text{H}_2\text{O}$  fluxes at individual tree and entire ecosystem levels and to estimate the contributions of soil, forest understorey, and various tree species of overstorey into total ecosystem fluxes while taking into account individual biophysical properties and responses of tree species to changes in environmental conditions. The model also allows taking into account the non-steady-state water transport in the trees, rainfall interception, dew generation, turbulence and convection flows within the canopy and plant canopy energy storage (Olchev et al. 2015).

## Data analysis

To estimate the possible impacts of ENSO events on energy, water, and  $\text{CO}_2$  fluxes in the tropical rainforest at the Bariri site the meteorological and flux data measured in the periods from 2003 to 2008 and from 2013 to 2017 were analyzed. The periods were chosen due to the small amount of gaps in the time series data. The period between 2003 and 2008 contains several warm ENSO events of moderate intensity. The period 2013–2017 contains one of the strongest warm events during the last several decades – the El Niño of 2015–16.

Statistical analysis included both simple correlation and cross-correlation analysis (Chatfield 2004). Correlation coefficients are calculated between the Niño4 index and the deviations of smoothed mean monthly (moving average  $\pm 3$  months) values of meteorological parameters and atmospheric fluxes from their monthly averages over the entire considered period (2003–2008, 2013–2017). The deviations were calculated according to the approach

described by Olchev et al (2015). Cross-correlation analysis was used to take into account possible forward and backward time shifts of maximal anomalies of meteorological parameters and energy, water, and CO<sub>2</sub> fluxes in respect to time of the El Niño culmination.

## RESULTS AND DISCUSSION

The El Niño event of 2015–2016 was one of the strongest ever recorded with the amplitude comparable to the extreme events of 1982–1983 and 1997–1998 (Santoso et al. 2017). The values of Niño3 and Niño4 indices reached in 2015–2016 values of 2.65°C and 1.59°C, respectively, that exceeds the corresponding values of SST anomalies observed in 1982–83 and 1997–98 for Niño4 region (Fig. 2c). Reanalysis data show that the area of positive anomalies of SST persisted over the Central and Eastern Pacific from June 2015 up to May 2016 and it was associated with strong westerly wind anomalies spreading up to 120°W in the ENSO culmination phase (Fig. 2a).

The extreme SST and atmosphere circulation anomalies induced a strong remote response over the entire equatorial Pacific region and resulted in significant changes in temperature and precipitation fields. In

the area of our study site in Central Sulawesi, Indonesia, this episode was manifested in positive temperature anomalies that exceeded 1°C during the culmination phase and it remained above the mean until the fall season of 2016 (Fig. 3c-d). Decreased precipitation over Sulawesi was observed from April 2015 to February 2016 (Fig. 3e-f). Similar trends were also revealed from data obtained at Bariri site (Fig. 4a-b). The easterly shift of the convection zone resulted also in higher solar radiation over Indonesia during summer and fall of 2015 and winter of 2015–2016 with a maximum in the period from September to November 2015 (Fig. 3a, 4a).

The comparisons of the 2013–17 time series of the mean monthly deviations of meteorological parameters measured at the tower in Bariri with anomalies calculated for the study area from reanalysis data showed that the deviations of solar radiation, air temperature and precipitation in 2015–16 from the mean values observed during the entire period of instrumental measurements at the experimental site are very well correlated with the anomalies obtained from reanalysis. From March 2015 up to October 2016 air temperature ( $T$ ) exceeded the mean temperature of 2003–2017 (Fig. 5a). Precipitation ( $P$ ) remained lower than

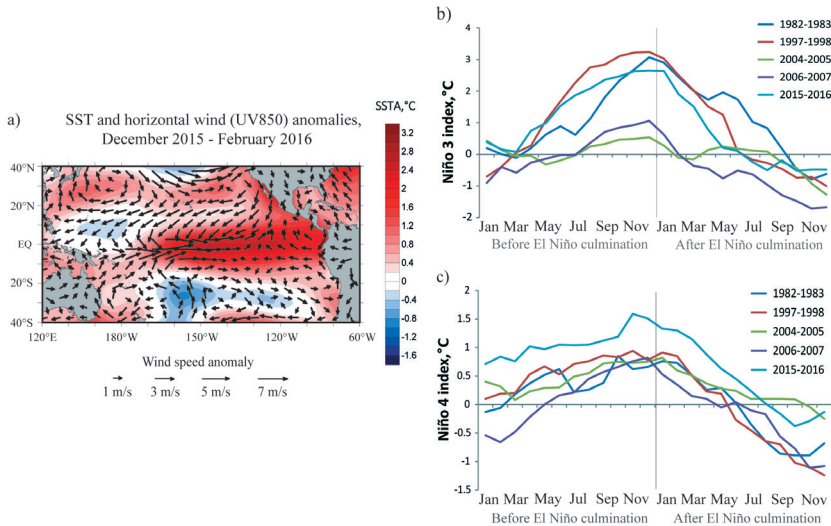


**Fig. 2. (a) Anomalies of sea surface temperature and wind at 850 hPa for the culmination phase of the El Niño 2015/2016 (December 2015 - February 2016), (b) the Niño3 index, and (c) the Niño4 index evolution during the strongest El Niño events since 1980s**

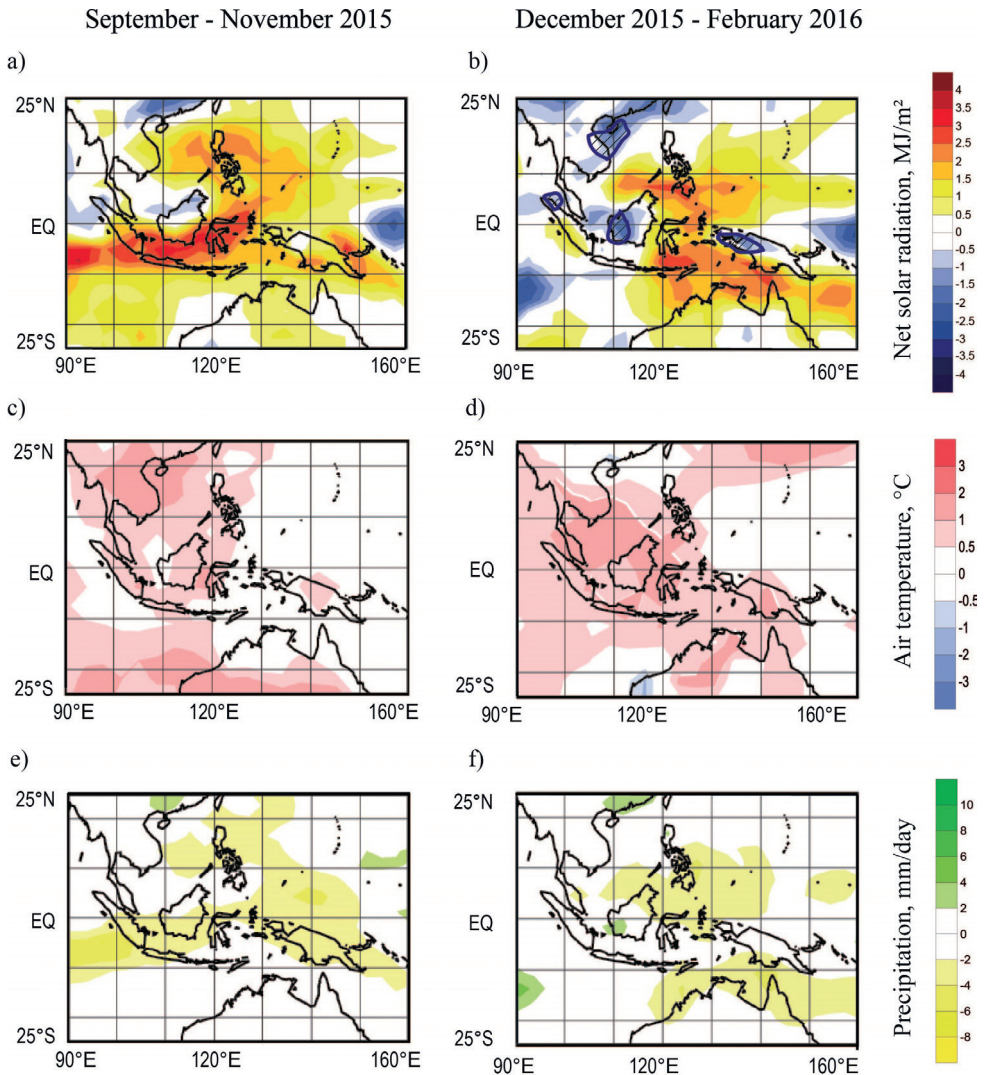


**Fig. 3. Anomalies of (a, b) surface net solar radiation, (c, d) near-surface air temperature and (e, f) precipitation during the development (left panel) and the peak (right panel) of the El Niño 2015/2016**

the mean values until November 2015 and exceeded them in the El Niño culmination phase (Fig. 5b). The temporal variability of water vapor pressure ( $e$ ) is characterized by insignificant variations during the El Niño development that are interrupted shortly before the El Niño peak and manifested in a fast growth of  $e$  simultaneously with  $P$  increasing (Fig. 4b,5b). The deviations of incoming solar radiation ( $G$ ) and net radiation ( $Rn$ ) from mean values have two peaks before and after El Niño culmination: in August-September 2015 and March-April 2016, respectively (Fig. 5a,e).

Monthly  $NEE$  and  $RE$  rates increase during the El Niño development, and the deviations from the means reached their maximum values almost simultaneously with the peak of the event (Fig. 5c-d). NPP exhibits negative anomalies during the El Niño of 2015–2016, while GPP shows a small, but consistent growth during the whole period from 2013 to 2017 (Fig. 4c-d, 5c-d). LE rate reaches maximum values about two months prior to the El Niño peak and suddenly decreases in the culmination and decaying phases (Fig. 4e, 5e). It can be explained by joint effects of positive cor-

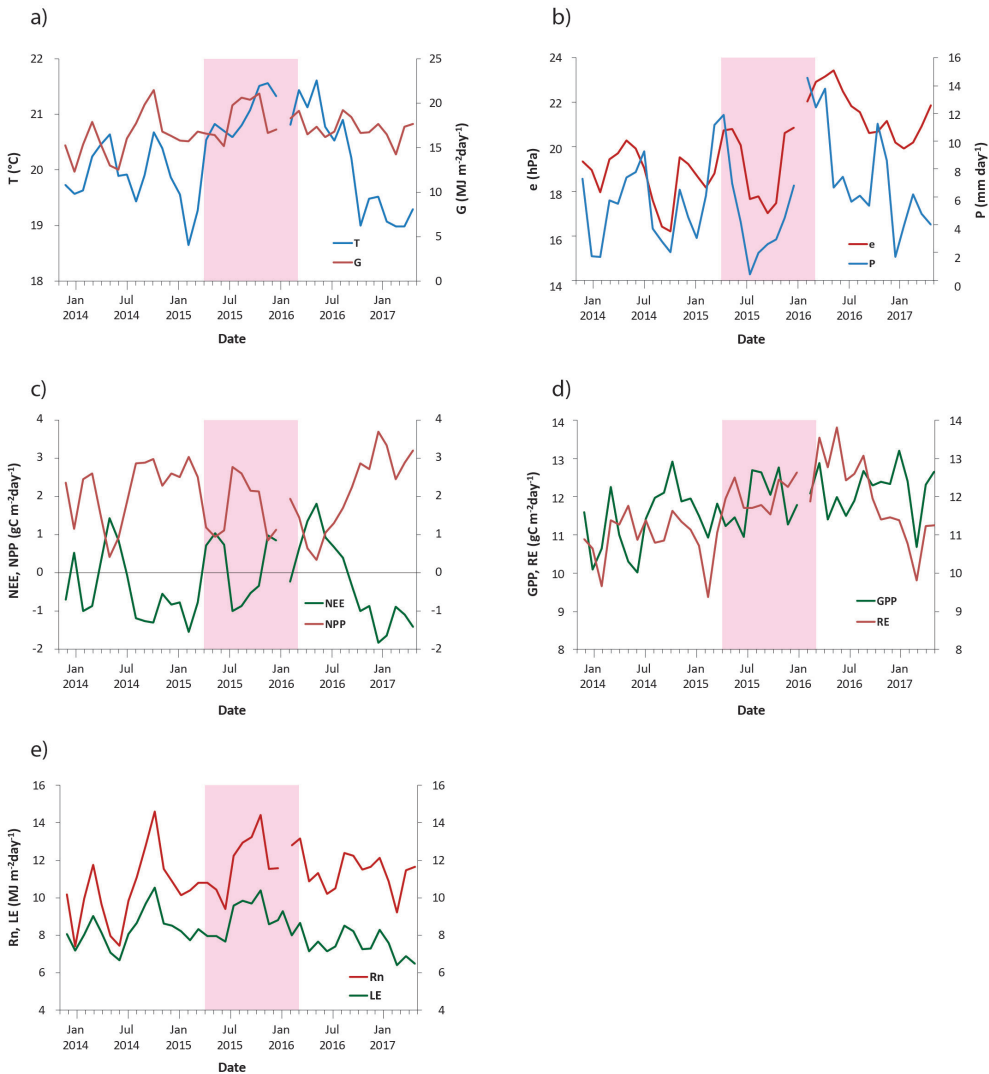


**Fig. 4.** Temporal variability of (a)  $T$  (°C) and  $G$  ( $\text{MJ m}^{-2} \text{day}^{-1}$ ), (b)  $e$  (hPa) and  $P$  ( $\text{mm day}^{-1}$ ), (c)  $NEE$  ( $\text{gC m}^{-2} \text{day}^{-1}$ ) and  $NPP$  ( $\text{gC m}^{-2} \text{day}^{-1}$ ), (d)  $GPP$  ( $\text{gC m}^{-2} \text{day}^{-1}$ ) and  $RE$  ( $\text{gC m}^{-2} \text{day}^{-1}$ ), (e)  $R_n$  ( $\text{MJ m}^{-2} \text{day}^{-1}$ ) and  $LE$  ( $\text{MJ m}^{-2} \text{day}^{-1}$ ) for the measurement period from December 2013 to April 2017 at the Bariri site. Pink rectangle indicates the period of the El Niño (Niño4  $>1.0^\circ\text{C}$ ) from April 2015 to March 2016

relations of  $\Delta LE$  with  $\Delta T$  ( $r=0.64$ ,  $p<0.05$ ) and with  $\Delta G$  ( $r=0.49$ ,  $p<0.05$ ) as well as of negative correlation of  $\Delta LE$  with  $\Delta e$  ( $r=-0.48$ ,  $p<0.05$ ).

In order to analyze the response of energy and  $\text{CO}_2$  fluxes in the tropical rainforest in Central Sulawesi to ENSO associated anomalies a lag cross correlation analysis is provided (Fig. 6). The cross-correlation analysis shows that  $NEE$  and  $RE$  rates have similar relationship with ENSO indices: they are neg-

atively correlated before and positively correlated after El Niño peak with maximum at -9 and 4 month lags, respectively. Therefore,  $NEE$  and  $RE$  are suppressed during the El Niño development phase and intensified after the ENSO culmination. The latter may be considered as a response to the high air temperature observed during the El Niño culmination phase (the maximum positive correlation of  $\Delta T$  with Niño4 index falls on the same time lag as for  $\Delta RE$ ). Taking into account that  $GPP$  is not influenced by the

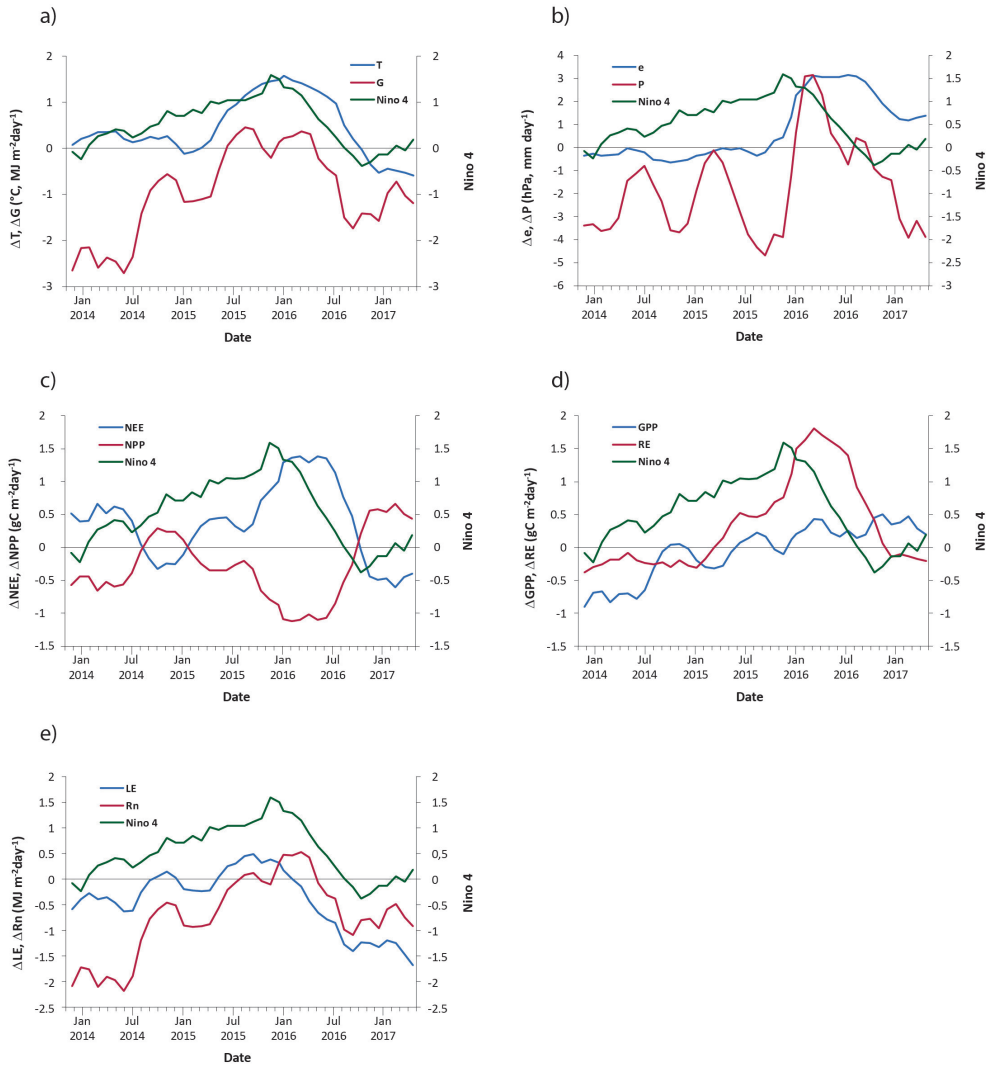


**Fig. 5. Deviations from 2003–2017 means of  $T$  ( $\Delta T$ ,  $^{\circ}\text{C}$ ),  $G$  ( $\Delta G$ ,  $\text{MJ m}^{-2} \text{day}^{-1}$ ),  $P$  ( $\Delta P$ ,  $\text{mm day}^{-1}$ ),  $e$  ( $\Delta e$ ,  $\text{hPa}$ ),  $LE$  ( $\Delta LE$ ,  $\text{MJ m}^{-2} \text{day}^{-1}$ ),  $Rn$  ( $\Delta Rn$ ,  $\text{MJ m}^{-2} \text{day}^{-1}$ ),  $GPP$  ( $\Delta GPP$ ,  $\text{gC m}^{-2} \text{day}^{-1}$ ),  $RE$  ( $\Delta RE$ ,  $\text{gC m}^{-2} \text{day}^{-1}$ ),  $NEE$  ( $\Delta NEE$ ,  $\text{gC m}^{-2} \text{day}^{-1}$ ) and  $NPP$  ( $\Delta NPP$ ,  $\text{gC m}^{-2} \text{day}^{-1}$ ) values at the Bariri site and SST anomalies in Niño4 region ( $^{\circ}\text{C}$ )**

El Niño of 2015–2016 in a straightforward manner and  $\Delta GPP$  is not correlated with Niño4, a relatively high correlation of  $\Delta NEE$  with Niño4 can be explained by a prevailing contribution of  $RE$  change into  $NEE$  variability. The temperature variation is connected in turn with solar radiation anomalies that preceded the air temperature anomaly by 3 months and reached their maximum at the El Niño peak. The same relationships with Niño4 index are observed for  $\Delta e$  and  $\Delta P$  values suggesting that anomalously high temperature during 2015–2016 El

Niño acts as a major influencing factor of observed anomalous conditions. The  $LE$  anomalies are mostly governed by changes of solar radiation which is supported by the same lag-correlation functions for  $\Delta G$  and  $\Delta LE$ .

Analysis of temporal variability of  $\Delta NPP$  shows that it changed in an opposite phase with  $\Delta NEE$ ,  $\Delta GPP$  and  $\Delta RE$  (Fig. 5, 6).  $\Delta NPP$  is positively correlated with Niño4 before the El Niño appearance and negatively correlated at El Niño culmination and its decaying



phases. Notably  $\Delta NPP$  is also in antiphase with temperature changes. The temporal variability of  $NPP$  usually coincides with the  $GPP$  pattern and is mainly influenced by  $G$  and  $T$  variability. It is likely that the  $\Delta NPP$  reduction after El Niño culmination can be explained, on the one hand, by a very low sensitivity of  $GPP$  of the tropical rainforest to changes of Niño4 index in the period of the El Niño of 2015–2016 and, on the other hand, by high contribution of  $T$  variations to the changes of forest canopy autotrophic respiration.

The El Niño of 2015–2016 was classified as a conventional event with some features of Modoki at the mature phase (Osipov and Gushchina 2018). In this context we compared the responses of energy, water and  $CO_2$  fluxes to the El Niño event of 2015–16

with flux anomalies observed during the moderate El Niños of 2004–05 and 2006–07 which were classified as Modoki events.

Comparison results show that the correlation of  $\Delta G$  and  $\Delta Rn$  with Niño4 index are quite similar for both periods, however in 2003–08 the  $\Delta G$  and  $\Delta Rn$  leads Niño4 by 3 months while in 2013–17 they are almost varied in the same phase. This is due to the fact that  $Rn$  and  $G$  growth during Modoki events occurs earlier in the seasonal cycle as compared to the conventional ENSO event. The  $\Delta LE$  variability is mainly influenced by solar radiation changes, and therefore has a similar pattern for both periods. Maximum correlation between  $\Delta LE$  and Niño4 index in 2003–08 is observed 2 months prior El Niño culmination and its response to Niño4 well agreed with re-

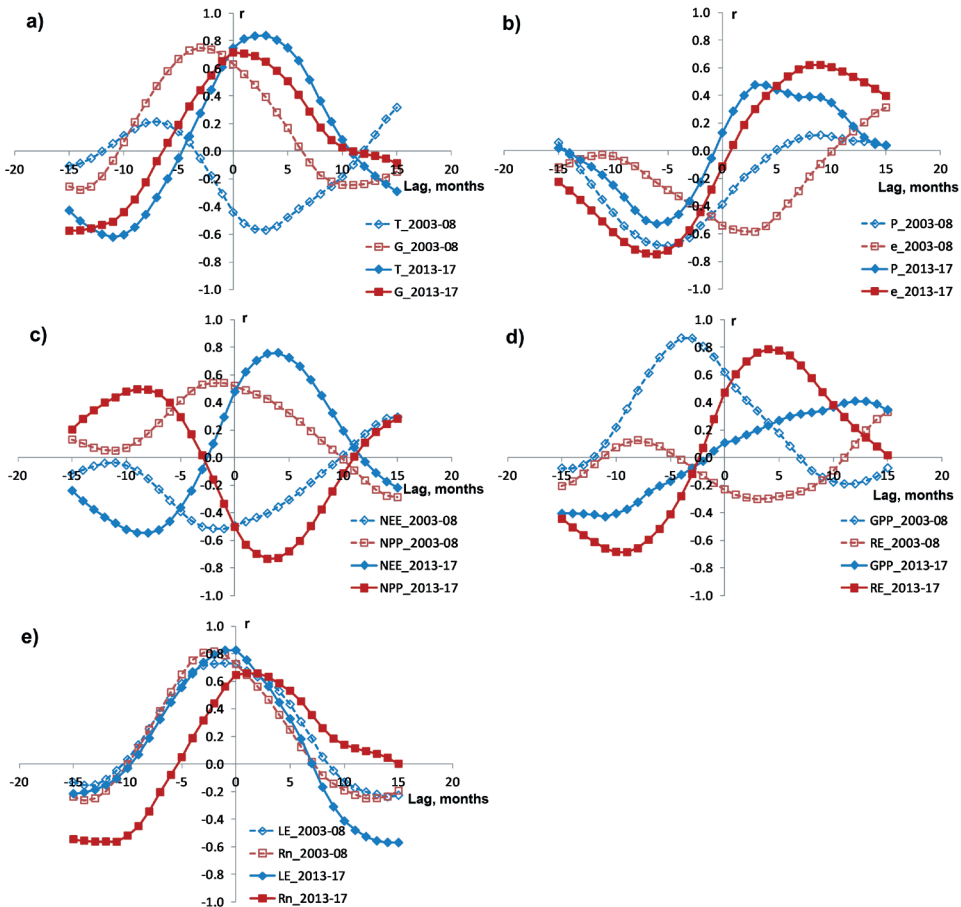


**Fig. 6. Cross-correlation ( $r$ ) functions between  $\Delta T$ ,  $\Delta G$ ,  $\Delta P$ ,  $\Delta e$ ,  $\Delta LE$ ,  $\Delta Rn$ ,  $\Delta GPP$ ,  $\Delta RE$ ,  $\Delta NEE$  and  $\Delta NPP$  values and Niño4 index. Solid lines – correlation for period from 2013 to 2017, dashed lines for 2003–2008 period**

sponses of  $Rn$  and  $G$  to Niño4 oscillations. Precipitation is strongly suppressed before El Niño peaks and increases after its culmination for all observed events. Noteworthy a weaker positive correlation between precipitation and Niño4 was observed in 2003–08 as compared to 2013–17. This effect may result from different decaying rate of conventional and Modoki events. The 2015–16 event decayed very quickly and passed to La Niña conditions, associated with extremely high precipitation in the western Pacific, in spring 2016. Whereas the Modoki events (observed in period 2003–08) are usually characterized by a longer decaying phase.

In contrast to solar radiation the air temperature and water vapor pressure anomalies are differently correlated with Niño4 index in 2003–08 and 2013–17 periods. The  $\Delta T$  values follow the  $\Delta G$  growth in 2015–16 and they are positively correlated with Niño4, while during Modoki events of 2003–08 the  $T$  deviations were always negative and did not exceed  $-0.5^\circ\text{C}$  (Oltchev et al. 2015). This led to the negative  $\Delta T$  and Niño4 correlation during the entire period of 2003–08 (Fig. 6). As a consequence,  $\Delta RE$  in 2003–08 was predominantly negative and was negatively correlated with Niño4. Very high correlation of  $\Delta GPP$  and Niño4, and very weak negative correlation of  $\Delta RE$  and Niño4 resulted in a clearly manifested negative correlation of  $\Delta NEE$  and Niño4 in 2003–08 in contrast to the period from 2013 to 2017, that is characterized by a very weak correlation between  $\Delta GPP$  and Niño4 and in turn a very well manifested positive correlation between  $\Delta NEE$  and Niño4 (Fig. 6). The difference in temporal patterns of  $\Delta e$  and Niño4 index in 2003–08 and 2013–17 could result from various air temperature and precipitation responses to the SST oscillation in Niño4 region.

The  $NPP$  and  $RE$  responses to the El Niño event are also strongly different in periods of 2003–08 and 2013–17. In 2003–08  $NPP$  is mainly influenced by  $\Delta G$ , which was tightly related to Niño4 variability whereas the temperature changes during this period were relatively low causing the small sensitivity of  $NPP$  to temperature. In 2015–16

we observed a weak dependence of  $\Delta GPP$  on Niño4 which resulted in a prevailing dependence of  $\Delta NPP$  on  $T$  oscillations and, as it was already mentioned, in a negative correlation between  $\Delta NPP$  and Niño4 at culmination and mature phases of the El Niño 2015–16. The different responses of  $\Delta RE$  to Niño4 changes are influenced by different effects of various types of ENSO of different intensity on the pattern of  $\Delta T$  in equatorial Pacific. The El Niño 2015–16 is characterized by a clearly manifested dependence of  $\Delta T$  on Niño4 variation whereas in the period from 2003 to 2008 such relation is insignificant.

The present study focuses on the analysis of possible effects of the 2015–16 El Niño event on the temporal variability of key meteorological parameters and energy, water, and  $\text{CO}_2$  fluxes in a tropical rainforest ecosystem. Possible uncertainties of flux estimations provided by the eddy covariance technique (caused by e.g. low turbulence, rainfall events, etc.) were not considered. To derive the flux responses to El Niño intensity we analyze monthly flux deviations from long-term mean fluxes obtained at the experimental site since 2003. Effect of flux measurement uncertainties on monthly flux deviations in this case is relatively small and can be neglected.

## CONCLUSIONS

The results of long-term eddy covariance flux measurements in a tropical rainforest in Central Sulawesi showed a very strong influence of the El Niño event of 2015–16 on local and regional meteorological conditions, energy, water, and  $\text{CO}_2$  fluxes. The El Niño influence is manifested in a strong increase of incoming solar radiation, low precipitation, and high air temperature that reach their maximum values quite simultaneously with the Niño4 index. Monthly precipitation reached maximum about 3–4 months after El Niño culmination. Increased incoming solar radiation, net radiation and surface temperature resulted in a strong increase of  $LE$  (surface evapotranspiration) that reached its maximum about two months before the El Niño peak.  $RE$  showed a continuous increase simultane-

ously with air temperature growth resulting in a positive anomaly of *NEE* (reduced  $\text{CO}_2$  uptake). The *GPP* rate is characterized by a very low sensitivity to Niño4 changes and had no impact on *NEE* rates. Low sensitivity of *GPP* to Niño4 also resulted in a negative anomaly of *NPP* that varied in reversed phase with *NEE*.

The discovered tropical rainforest responses (key meteorological parameters as well as energy, water, and  $\text{CO}_2$  fluxes) to the El Niño 2015–16 forcing are different from the ones during the moderate El Niño events of 2003–08. The main difference is the strong relationship between air temperature and Niño4 index during 2015–16 that was not observed during 2003–08. As a consequence, the sensitivity of *RE* to Niño4 during the period of 2003–08 was very low in contrast to the well manifested dependence of *RE* on Niño4 during the period of 2015–16. High *RE* was the main driver of  $\text{CO}_2$  uptake reduction (decrease of *NEE*), as well as decrease of *NPP* during the El Niño phenomenon of 2015–16. No differences in relationships between *LE* and Niño4 for the analyzed periods with El Niño of different intensities were found. It can be assumed that the different sensitivity of the energy, water, and  $\text{CO}_2$  fluxes of

the tropical rainforest ecosystem to El Niño events is due to various intensity of meteorological anomalies that were observed in the region during the considered period. It can be expected that anomalies of key meteorological parameters (e.g. temperature, precipitation, solar radiation) with different intensity may result in opposite effects on the  $\text{CO}_2$  and energy fluxes.

## ACKNOWLEDGEMENTS

The study was supported by the German Research Foundation (DFG) under the projects "Stability of Rainforest Margins in Indonesia", STORMA (Collaborative German-Indonesian Research Center CRC 552), "Ecological and Socioeconomic Functions of Tropical Lowland Rainforest Transformation Systems (Sumatra, Indonesia)" (Collaborative German-Indonesian Research Center CRC 990) and "BaririFlux" (KN 582/8-1), as well as by Lomonosov Moscow State University (grant No. AAAA-A16-116032810086-4). The authors would like to thank Pak Dudin, Pak Ore, Ibu Aiyen Tjoa, Dietmar Fellert and Edgar Tunsch for assistance with field measurements. ■

## REFERENCES

- Alisov B.P. (1954). *Die Klimate der Erde*. Berlin: Deutscher Verlag der Wissenschaften. 277 pp.
- Aubinet M., Vesala T. and Papale D. (2012). *Eddy covariance. A practical guide to measurement and data analysis*. Springer. 438 pp.
- Ashok K., Behera S. K., Rao S. A., Weng H., Yamagata T. (2007). El Niño Modoki and its possible teleconnection. *Journal of Geophysical Research*, 112, C11007.
- Chatfield C. (2004). *The Analysis of Time series, An Introduction*, 6th ed. New York: Chapman & Hall/CRC, 333 pp.
- Chen D. and Chen H.W. (2013) Using the Koppen classification to quantify climate variation and change: An example for 1901–2010. *Environmental Development*, 6, pp. 69–79
- Ciais P., Piao S.-L., Cadule P., Friedlingstein P., and Chedin A. (2009). Variability and recent trends in the African terrestrial carbon balance. *Biogeosciences*, 6, pp. 1935–1948.
- Corlett R., Primack R. (2006). Tropical rainforests and the need for cross-continental comparisons. *Trends in Ecology and Evolution*, 21 (2), pp. 104–110.

Grace J., Lloyd J., McIntyre J., Miranda A., Meir P., Miranda H., Nobre C., Moncrieff J.B., Massheder J.M., Malhi Y., Wright I. and Gash J.C. (1995). Carbon dioxide uptake by an undisturbed tropical rain forest in south-west Amazonia, 1992 to 1993. *Science*, 270, pp. 778-780.

Dee D.P., Uppala S.M., Simmons A.J., Berrisford P., Poli P., Kobayashi S., Andrae U., Balmaseda M.A., Balsamo G., Bauer P., Bechtold P., Beljaars A.C.M., van de Berg L., Bidlot J., Bormann N., Delsol C., Dragani R., Fuentes M., Geer A.J., Haimberger L., Healy S.B., Hersbach H., Hólm E.V., Isaksen I., Kållberg P., Köhler M., Matricardi M., McNally A.P., Monge-Sanz B.M., Morcrette J.-J., Park B.-K., Peubey C., de Rosnay P., Tavolato C., Thépaut J.-N., Vitart F. (2011). The ERA-Interim reanalysis: configuration and performance of the data assimilation system. *Quarterly Journal of the Royal Meteorological Society*, 137(656), pp. 553–597. <https://doi.org/10.1002/qj.828>.

Dewitte B., Gushchina D., du Penhoat Y., Lakeev S. (2002). On the importance of subsurface variability for ENSO simulation and prediction with intermediate coupled models of the tropical Pacific: A case study for the 1997-1998 El Niño. *Geophysical Research Letters*, 29(14). <https://doi.org/10.1029/2001GL014452>.

Diaz H.F., Hoerling M.P., and Eischeid J. K. (2001). ENSO variability, teleconnections and climate change. *Int. J. Climatol.*, 21, pp.1845– 1862, <https://doi.org/10.1002/joc.631>.

Falk U., Ibrom A., Kreilein H., Oltchev A., Gravenhorst G. (2005). Energy and water fluxes above a cacao agroforestry system in Central Sulawesi, Indonesia, indicate effects of land-use change on local climate. *Meteorologische Zeitschrift*, 14(2), pp. 219-225.

Feely R.A., Wanninkhof R., Takahashi T., and Tans P. (1999). Influence of El Niño on the equatorial Pacific contribution to atmospheric CO<sub>2</sub> accumulation. *Nature*, 398, pp. 597-601.

Food and Agriculture Organization of the United Nations. *Global Forest Resources Assessment 2015: How are the world's forests changing? (Second Edition)*. (2016). Rome. 54 pp.

Grace J., Lloyd J., McIntyre J., Miranda A.C., Meir P., Miranda H.S., Nobre C., Moncrieff J., Massheder J., Malhi Y., Wright I., Gash J. (1995). Carbon dioxide uptake by an undisturbed tropical rain forest in Southwest Amazonia, 1992 to 1993. *Science*, 270(5237), pp. 778-780.

Gushchina D.Y., Petrosyants M.A., Semenov E.K. (1997). An empirical model of tropical tropospheric circulation during ENSO. part II. Analysis of evolution of circulation characteristics. *Russian Meteorology and Hydrology*, 2, pp. 8–18.

Hansen M.C., Potapov P.V., Moore R., Hancher M., Turubanova S.A., Tyukavina A., Thau D., Stehman S.V., Goetz S.J., Loveland T.R., Kommareddy A., Egorov A., Chini L., Justice C.O., Townshend J.R.G. (2013). High-Resolution Global Maps of 21st-Century Forest Cover Change. *Science*, vol. 342 (6160), pp. 850-853. <https://doi.org/10.1126/science.1244693>.

Hirano T., Segah H., Harada T., Limin S., June T., Hirata R., Osaki, M. (2007) Carbon dioxide balance of a tropical peat swamp forest in Kalimantan, Indonesia. *Glob. Change Biol.*, 13, pp. 412–425.

Huffman G.J., Adler R.F., Bolvin D.T., Gu G. (2009). Improving the global precipitation record: GPCP Version 2.1. *Geophys. Res. Lett.*, 36, L17808. <https://doi.org/10.1029/2009GL040000>.

Ibrom A., Olchev A., June T., Ross T., Kreilein H., Falk U., Merklein J., Twele A., Rakkibu G., Grote S., Rauf A. and Gravenhorst G. (2007). Effects of land-use change on matter and energy exchange between ecosystems in the rain forest margin and the atmosphere. In *The stability of tropical rainforest margins: Linking ecological, economic and social constraints*. Eds. Tschardt T., Leuschner C., Zeller M., Guhardja E. and Bidin A., Springer Verlag, Berlin, pp. 463 – 492.

Ibrom A., Oltchev A., June T., Kreilein H., Rakkibu G., Ross Th., Panferov O., Gravenhorst G. (2008) Variation in photosynthetic light-use efficiency in a mountainous tropical rain forest in Indonesia. *Tree Physiol.*, 28, pp. 499–508

Ichii K., Ueyama M., Kondo M., Saigusa N., Kim J., Alberto M.C., Ardö J., Euskirchen E.S., Kang M., Hirano T., Joiner J., Kobayashi H., Marchesini L.B., Merbold L., Miyata A., Saitoh T.M., Takagi K., Varlagin A., Bret-Harte M.S., Kitamura K., Kosugi Y., Kotani A., Kumar K., Li S.G., Machimura T., Matsuura Y., Mizoguchi Y., Ohta T., Mukherjee S., Yanagi Y., Yasuda Y., Zhang Y., Zhao F. (2017). New data-driven estimation of terrestrial CO<sub>2</sub> fluxes in Asia using a standardized database of eddy covariance measurements, remote sensing data, and support vector regression. *Journal of Geophysical Research Biogeosciences*, 122, pp. 767–795.

Le Quéré C., Moriarty R., Andrew R.M., Peters G.P., Ciais P., Friedlingstein P., Jones S.D., Sitch S., Tans P., Arneeth A., Boden T.A., Bopp L., Bozec Y., Canadell J.G., Chevallier F., Cosca C.E., Harris I., Hoppema M., Houghton R.A., House J.I., Jain A., Johannessen T., Kato E., Keeling R.F., Kitidis V., Klein Goldewijk K., Koven C., Landa C.S., Landschützer P., Lenton A., Lima I.D., Marland G., Mathis J.T., Metzl N., Nojiri Y., Olsen A., Ono T., Peters W., Pfeil B., Poulter B., Raupach M.R., Regnier P., Rödenbeck C., Saito S., Salisbury J.E., Schuster U., Schwinger J., Séférian R., Segsneider J., Steinhoff T., Stocker B.D., Sutton A.J., Takahashi T., Tilbrook B., van der Werf G.R., Viovy N., Wang Y.-P., Wanninkhof R., Wiltshire A., Zeng N. (2015). Global carbon budget 2014. *Earth System Science Data*, 7(1), pp. 47–85.

Malhi Y., Mateus J., Migliavacca M., Misson L., Montagnani L., Moncrieff J., Moors E., Munger J.W., Nikinmaa E., Ollinger S.V., Pita G., Rebmann C., Rouspard O., Saigusa N., Sanz M.J., Seufert G., Sierra C., Smith M.-L., Tang J., Valentini R., Vesala T. and Janssens I.A. (2007). CO<sub>2</sub> balance of boreal, temperate, and tropical forests derived from a global database. *Global Change Biology*, 13(12), pp. 2509–2537.

Malhi Y. (2010). The carbon balance of tropical forest regions, 1990–2005. *Current Opinion in Environmental Sustainability*, 2(4), pp. 237–244.

Myers N., Mittermeier R.A., Mittermeier C.G., da Fonseca G.A.B., Kent J. (2000) Biodiversity hotspots for conservation priorities. *Nature*, 403, pp. 853–858. <https://doi.org/10.1038/35002501>.

Oltchev A., Cermak J., Nadezhkina N., Tatarinov F., Tishenko A., Ibrom A., Gravenhorst G. (2002). Transpiration of a mixed forest stand: field measurements and simulation using SVAT models. *Boreal Environmental Research*, 7(4), pp. 389–397.

Olchev A., Ibrom A., Ross T., Falk U., Rakkibu G., Radler K., Grote S., Kreilein H., Gravenhorst G. (2008). A modelling approach for simulation of water and carbon dioxide exchange between multi-species tropical rain forest and the atmosphere. *J. Ecological Modelling*, 212, pp. 122–130.

Olchev A., Ibrom A., Panferov O., Gushchina D., Kreilein H., Popov V., Propastin P., June T., Rauf A., Gravenhorst G., and Knohl A. (2015). Response of CO<sub>2</sub> and H<sub>2</sub>O fluxes in a mountainous tropical rainforest in equatorial Indonesia to El Niño events. *Biogeosciences*, 12, pp. 6655-6667.

Osipov A. and Gushchina D. (2018). El Nino 2015/2016: evolution, mechanisms, and concomitant remote anomalies. *Fundamental and applied climatology (in Russian)*, 3, pp. 54-81.

Panferov O., Ibrom I., Kreilein H., Oltchev A., Rauf A., June T., Gravenhorst G. and Knohl A. (2009). Between deforestation and climate impact: the Bariri Flux tower site in the primary montane rainforest of Central Sulawesi, Indonesia. *The Newsletter of FLUXNET*. 2(3), pp. 17-19.

Santoso A., McPhaden M.J., and Cai W. (2017). The defining characteristics of ENSO extremes and the strong 2015/2016 El Niño. *Reviews of Geophysics*, 55, pp. 1079–1129. <https://doi.org/10.1002/2017RG000560>.

Trenberth K.E., Branstator G.W., Karoly D., Kumar A., Lau N.-C., and Ropelewski C. (1997). The definition of El Niño. *Bulletin of the American Meteorological Society*, 78(12), pp. 2771-2777.

Zheleznova I.V., Gushchina D.Y. (2015). The response of global atmospheric circulation to two types of El Niño. *Russian Meteorology and Hydrology*, 40(3), pp. 170-179.

Zheleznova I. V., Gushchina D. Y. (2016). Circulation anomalies in the atmospheric centers of action during the Eastern Pacific and Central Pacific El Niño. *Russian Meteorology and Hydrology*, 41 (11-12), pp. 760–769.

Received on December 31<sup>st</sup>, 2018

Accepted on May 17<sup>th</sup>, 2019